Rivista Italiana di Paleontologia e Stratigrafia
(*Research in Paleontology and Stratigraphy*)
vol. 126(3): 847-864. **November 2020**

THE MICROFACIES, SEQUENCE STRATIGRAPHY AND GENESIS OF THE UPPER DEVONIAN PHOSPHORITES IN THE NORTH OF KERMAN, SE IRAN

MOHAMMAD JAVAD HASSANI[1*], HAMED AMERI[1], MEHDI HONARMAND[1] & FATEMEH HOSSEINIPOUR[2]

[1]Department of Ecology, Institute of Science and High Technology and Environmental Sciences, Graduate University of Advanced Technology, End of Haftbagh Highway, Kerman, Iran.
[2]Department of Geology, Payame Noor University (PNU), Tehran, Iran.
*Corresponding author, e-mail: mjhassani887@gmail.com

To cite this article: Hassani M.J., Ameri H., Honarmand M. & Hosseinipour F. (2020) - The microfacies, sequence stratigraphy and genesis of the upper Devonian phosphorites in the north of Kerman, SE Iran. *Riv. It. Paleontol. Strat.*, 126(3): 847-864.

Keywords: Phosphorite; Devonian; Sequence stratigraphy; upwelling; Kerman.

*Abstract***.** This research focuses on the microfacies, sequence stratigraphy and genesis of the upper Devonian phosphate-rich deposits in the Kerman province, SE Iran. These deposits are investigated in the Sarashk and Hutk sections, which are the most complete upper Devonian strata in the studied area. This region was located on the northern coast of the Gondwanaland during the Devonian. Detailed sampling and sedimentological analyses indicate that the studied successions consist of limestone, shale and sandstone lithofacies. The limestone lithofacies includes 12 microfacies and the shale and sandstone lithofacies include two microfacies. Based on the microfacies analysis, five sedimentary sequences are distinguished in each section. The microfacies analyses suggest a mixed carbonate-siliciclastic ramp sedimentary environment. Based on the sequence stratigraphic settings, the phosphorite layers are divided into three types, the first involves lumachella strata and was deposited in transgressive system tract settings; the second was deposited in the high stand system tract and maximum flooding surface settings and the third includes the basal parts of the falling stage system tract setting. The first phosphorite type seems to be a direct result of upwelling currents and blooms in continental shelf deviling creatures, especially brachiopods and fishes. The second, and the most commercially qualified, type formed as an indirect result of upwelling currents and subsequent toxic waters, high mortality and rise of Oxygen Minimum Zone. The third type was a result of post deposition burial digenesis and cementation processes.

Introduction

Phosphorus (^{15}P) is a vital nutrient for living creatures; this element plays a fundamental rule in the DNA structure and ATP molecules (Pasek 2008; Goldhammer et al. 2011). As well as DNA and ATP, phosphorus is a critical component for many other biochemicals in plants and animals (Föllmi 1996; Pufahl & Groat 2016). Phosphorus is also used in fertilizers, feed additives, water and metal treatments, detergents, medicines, metallic products processing, food and drink processing, batteries and electronic devices and many other industrial processes and products (Pufahl & Groat 2016).

The world resources of phosphorus are estimated by the U.S. Geological Survey at ca. 300,000 Mt (Pufahl & Groat 2016), with 95% sedimentary and 5% igneous (Jasinski 2016). In general, sedimentary units with more than 18% P_2O_5 are

Received: November 9, 2019; accepted: October 20, 2020

called phosphorite, a marine biochemical sedimentary rock (Nelson et al. 2010), and could be use as phosphate resource. Although some deposits with 15% P_2O_5 and low contamination have been used for agricultural phosphatic fertilizers. The average of 0.071-0.372 ppm phosphorous content of seawater (Simandl et al. 2011) is inadequate for phosphogenesis directly. Although phosphate rich sedimentary layers may deposited everywhere, phosphorites are commonly deposited on passive margins with effective connection to the ocean in moderately temperate and near equatorial zones (between 40° N - 40° S), (Cook & McElhinny 1979; Simandl et al. 2011). The mechanism of deposition of phosphorites is uncertain in geological history (Föllmi 1996; Trappe 1998; Schulz & Schulz 2005; Dornbos 2010; Bailey et al. 2013). In some cases, igneous activities, such as volcanism and hydrothermal fluids, are assigned as the main source of phosphate enrichment (Berner 1973; Froelich et al. 1982; Wheat et al. 1996; Petsch & Berner 1998). Some researchers emphasize the role of microbial activities as a direct or indirect cause of phosphogenesis in sedimentary basins (Reimers et al. 1990; Schulz & Schulz 2005; Bailey et al. 2007; Barale et al. 2013; Lepland et al. 2013; Salama et al. 2015). In this case, the Sulphur-Oxidizing bacteria are the most important operatives and take part in phosphogenesis in some areas (Kazakov 1937; Burnett 1977; Reimers et al. 1990; Schulz & Schulz 2005; Bailey et al. 2007; Bailey et al. 2013; Lepland et al. 2013).

However, among phosphogenesis mechanisms, upwelling currents considered as the main mechanism for deposition of phosphate rich sediments in ancient and modern phosphorite factories worldwide (Burnett 1977; Baturin 1982; Goldhammer et al. 2010; Lass et al. 2010; Nelson et al. 2010; Goldhammer et al. 2011; Alsenz et al. 2015; Brandano et al. 2016; Lomnitz 2017). Upwelling currents carry oxygen and nutrient-rich waters up to the shallow and photic zone which leads to high productivity and blooms of various organisms, including plants and animals. The high productivity can be followed by toxic and anoxic waters and accumulation of organic matter in the continental margin sediments. One of the organic components concentrated is phosphorous, as bones and shells or minerals. The most common P mineral in the phosphorites is Francolite, an authigenic carbonate rich fluorapatite: $[Ca_{10-a-b}Na_aMg_b(PO_4)_{6-x}(CO_3)_{x-y-z}(CO_3{\cdot}F)_{x-y-z}(SO_4)_zF_2]$. This mineral contains 32% P_2O_5, 52%, CaO, and 4% F, and includes 1.2 ± 0.2% Na, 0.25 ± 0.02 % Sr, 0.36 ± 0.03 % Mg, 6.3 ± 0.3% CO2, and 2.7 ± 0.3% SiO_2 (Jarvis et al. 1994). Weathering and diagenesis may alter the francolite to Fe-rich (Strengite) or Al-rich (Crandallite, Millisite, Wavellite) phosphate minerals. However, the concentration of P_2O_5 in phosphorite layers could result from in situ mineralization of Francolite or reworked pellets, oolites, nodules or fragments of bones or shells. These deposits concentrated in transgressive-regressive cycles and the most valuable phosphorite layers were deposited in the Cambrian, Permian, Jurassic, Cretaceous, Eocene and Miocene (Simandl et al. 2011). Nevertheless, some phosphorite layers have deposited on the northern margin of Gondwanaland during the late Devonian and crop out on the Iranian plateau. The phosphorite layers in the Alborz Structural Zone are involved in the Geirud Formation (Salama et al. 2018) and are explored and exploited in the Geirud mine; but in the Central Iran Structural Zone (CISZ) the favorable layers are not explored yet. The major Devonian - Lower Carboniferous strata of southern Iran have been studied and reported by Wendt et al. (2002) and phosphate rich units in the upper Devonian strata are reported by them. Earlier, Dimitrijevic (1973) reported "phosphate Unit" in his studies in Kerman, but he did not study the geochemical and sedimentological characteristics of those units. The phosphorites of the some area were reported by Dastanpour (1996, 1999), but their origin and sedimentary environment were not investigated. This study deals with the sedimentology, sequence stratigraphy and geochemistry of phosphorite deposits in the north of Kerman in two localities, the Hutk and Sarashk areas, and presents their detailed sedimentological and geochemical characteristics.

Geological setting

The studied area, as a part of the CISZ (Berberian & King 1981), is located at the noth of Kerman Province, south-southeastern Iran (Fig. 1a). The upper Devonian strata at the north of Kerman outcrop mainly in two complicated mountainous areas. The Hutk Section is located close to Hutk Village at 56°56'42.34"E - 30°34'16.84"N, 32 Km north of

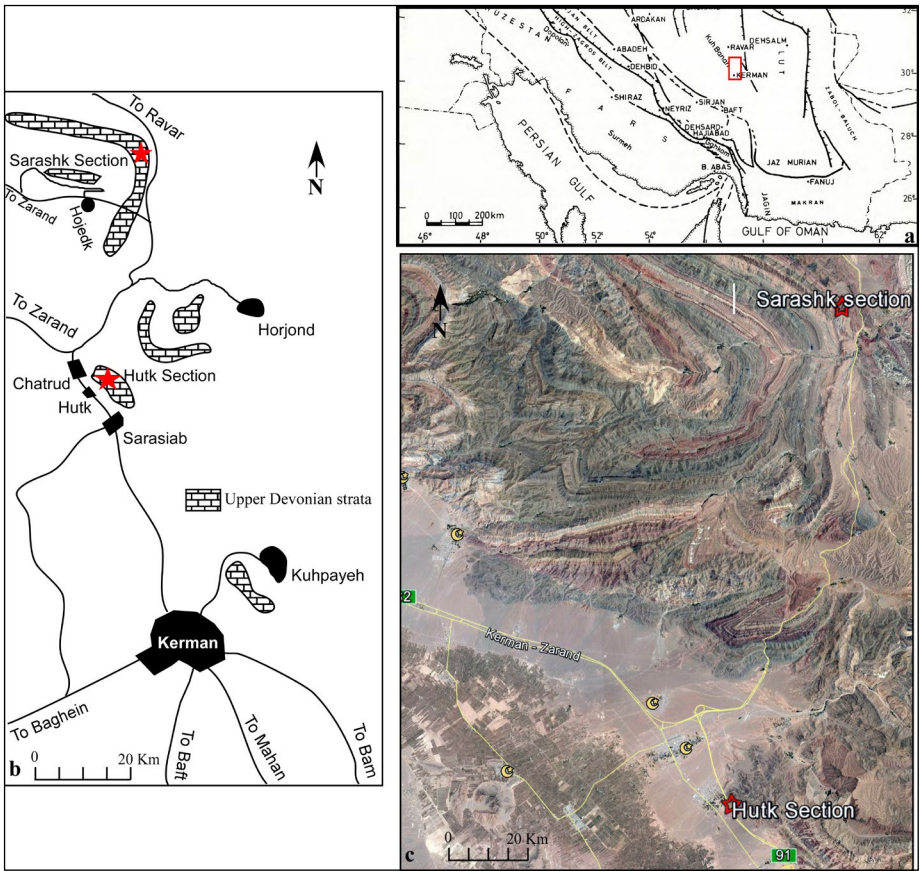

Fig. 1 - a) The location of the studied area in the south of Iran, after Berberian & King (1981); b) access map of the studied sections; c) satellite image of the studied area (from Google Earth).

Kerman, and the Sarashk Section is located 75 km north of Kerman at 57° 1'34.23"E - 30°50'16.74"N (Fig. 1b). Both sections have been measured in dark folded layers of the Middle – Late Paleozoic at the north of Kerman (Fig. 1c). The studied area was located on the northern margin of Gondwanaland in a tropical zone during the Middle Paleozoic (Wendt et al. 2002).

The main lithology of studied strata includes limestone and shale and minor sandstone, sandy limestone and dolomitic limestone intercalations. As well as limestone and shale, there are some reefal strata with various thicknesses in many localities. These deposits are classified by Wendt et al. (2002), in the Zone A (Fig. 2) as marine Devonian- Carboniferous deposits. Based on the field observations, the base and the top of studied strata are characterized by sharp lithological changes.

The biostratigraphy of the Devonian strata in Kerman Area has studied by some authors (Ahmadi et al. 2006; Gholamalian 2006; Gholamalian & Kebriaei 2008; Khosravi et al. 2010; Ahmadi et al. 2011; Bahrami et al. 2011; Gholamalian et al. 2013; Bahrami et al. 2014; Gholamalian et al. 2014; Gholamalian et al. 2015; Ahmadi et al. 2016) mainly based on conodonts. Gholamalian (2006) established a Middle to late Frasnian age based on the presence of *Polygnathus zinaidae* and *Icriodus vitabilis* for the basal parts of the Hutk section. He also established the Early Famenian for the upper part of the Hutk section based on the presence of *Polygnathus semicostatus, Icriodus cornutus, Icriodus iowaensis iowaensis* and *Pelekysgnathus Inclinatus*. The final layers of the Hutk section belongs to the Early Carboniferous (Tournasian), also based on conodonts (Ahmadi et al. 2016). The recovered conodont fauna of the Sarashk section by some authors (Ahmadi et al. 2011; Bahrami et al. 2014) indicates that the whole of the section belongs to the Late Devonian (Late Frasnian-Famennian).

Materials and methods

The Hutk section comprises 449 meters of sandstones, limestones, reefal limestones and shales and 103 samples were collected from the whole section. The Sarashk section consists of 365 meters of sandstones, dolomitized limestones, limestone, reefal limestones and shale-limestone intercalations and 105 samples were

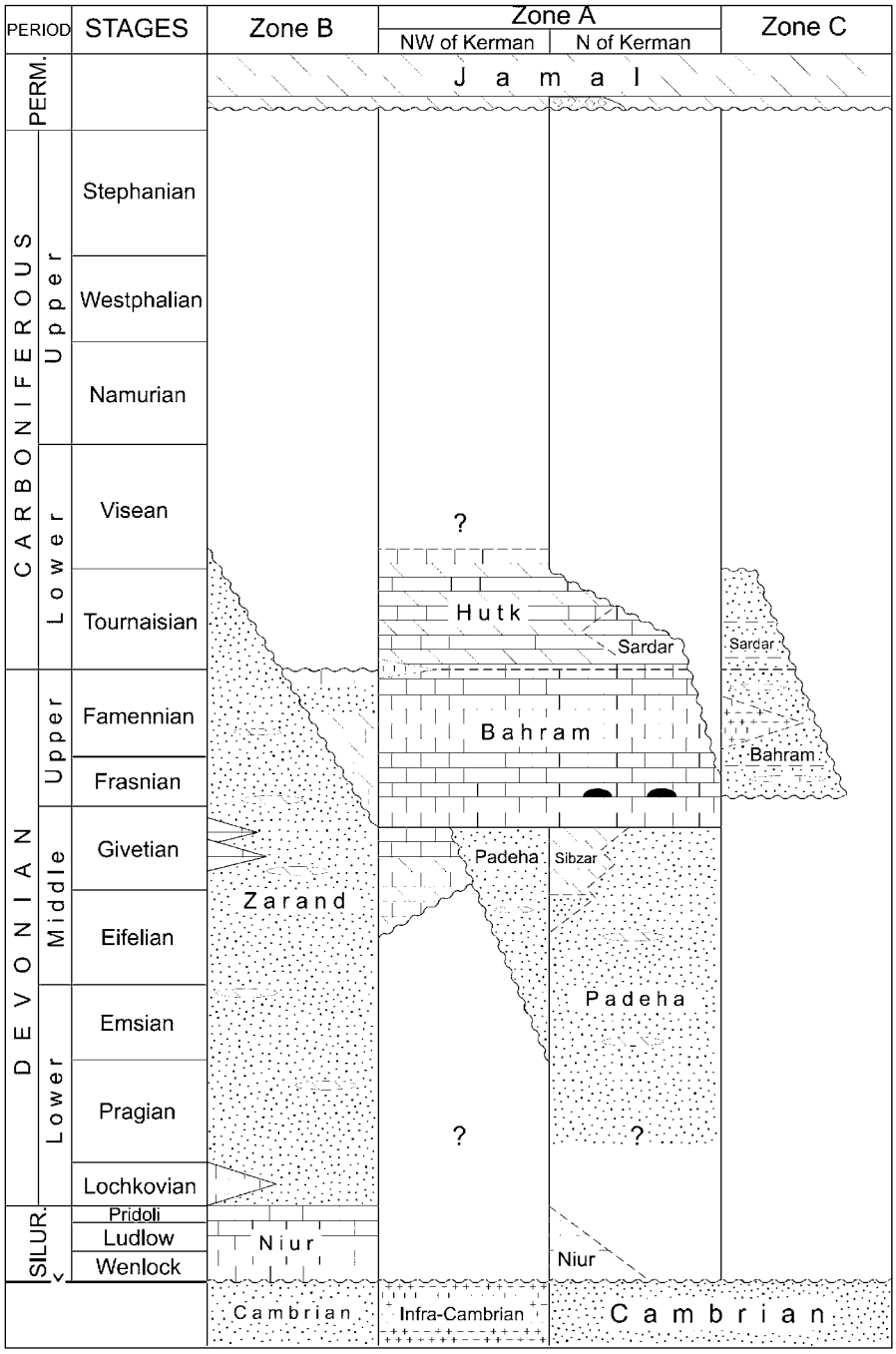

Fig. 2 - The main classification of the Devonian–Carboniferous strata in the Kerman Province. After Wendt et al. (2002).

collected from all strata. Both sections unconformably overlay older lower – middle Devonian strata of the Padeha Formation. The upper contact is unconformable and covered with the dolomitic strata of the Permian Jamal Formation. For microfacies studies, 162 thin sections were prepared from hard rock samples and studied using an Olympus polarizing microscope. The standard microfacies and sedimentary environment interpretations are based on common references (Wilson 1975; Flügel 2010; Flügel 2012). All loose and hard samples (except sandstones) were checked for P_2O_5 content by ammonium molybdate - nitric acid solution (Luternauer & Pilkey 1967; Swanson 1981; Adorno et al. 2016). Finally, 118 samples, which were marked as phosphate-bearing by the ammonium molybdate - nitric acid solution check, were analyzed for P_2O_5 concentration using LAB CENTER XRF-1800XRF instrument with 0.01% precision (Tab. 1 in Supplementary file).

Results and discussion

Sedimentology and sequence stratigraphy

The lithofacies and microfacies analyses of Hutk and Sarashk sections resulted in identification of a limestone lithofacies with 12 microfacies, a shale lithofacies with 2 microfacies and a sandstone lithofacies with 2 microfacies (Table 2). The structure, composition and grain size analyses of the identified facies were based on the classification of Flügle (2010, 2012) and Wilson (1975). Field observations showed a lack of oncoids, lack of extend-

Tab. 2 - Identified lithofacies and microfacies and their characteristics, SMF and Facies belts.

Lithology	Microfacies cod	Microfacies name	Allochemicals, structures, SMF & RMF (Flugel, 2010)	Facies belt (Flugel, 2010)
limestone	L1	Sandy intraclast bioclast wack/packstone	Sand + large to medium brachiopod & mollusc debris - SMF24, RMF24	Shallow Peritidal zones
	L2	Dolomitized lime mudstone	Rare bioclast remnants- SMF23, RMF19	Protected and low-energy inner ramp
	L3	Brachiopod bioclast wack/packstone	brachiopod shells molluscs + rare algae - SMF12,~ RMF18	
	L4	Peloid bioclast wack/packstone	Peloid, brachiopod + mollusc shells - SMF16, RMF16	
	L5	Algal Bioclast wack/packstone	Algae, brachiopod + bryozoan shells - SMF18, RMF17	
	L6	Oolite coated bioclast grainstone	Oolite + shell fragments - SMF11, RMF30	Sand shoals
	L7	Bioclast pack/grainstone	Brachiopods, algae, bryozoans, corals - SMF18, RMF13	Open inner ramp
	L8	Coral-algal rudstone	Algae + corals - SMF6, RMF15	
	L9	Coral framestone	Mainly Rugosa corals - SMF7, RMF12	Mid-ramp
	L10	Bafflestone	Mixed corals, rare stromatoporoids - SMF5, RMF9	
	L11	Crinoid echinoderm peloid wackestone	Crinoid debris + rare fine brachiopod shells - SMF4, RMF3	Outer ramp
	L12	Lime mudstone	10> crinoids and brachiopods - SMF3, RMF5	
shale	Sh1	Black organic rich shale	Peloids + shell debris	
	Sh2	Dark brown shale	Rare shell debris	Mid-outer ramp
sandstone	SS1	Quartzarenite	90%<well sorted quartz grains	Coastal, Inter-tidal
	SS2	Litharenite	Well rounded rock fragments + sub-rounded quartz grains	Supratidal

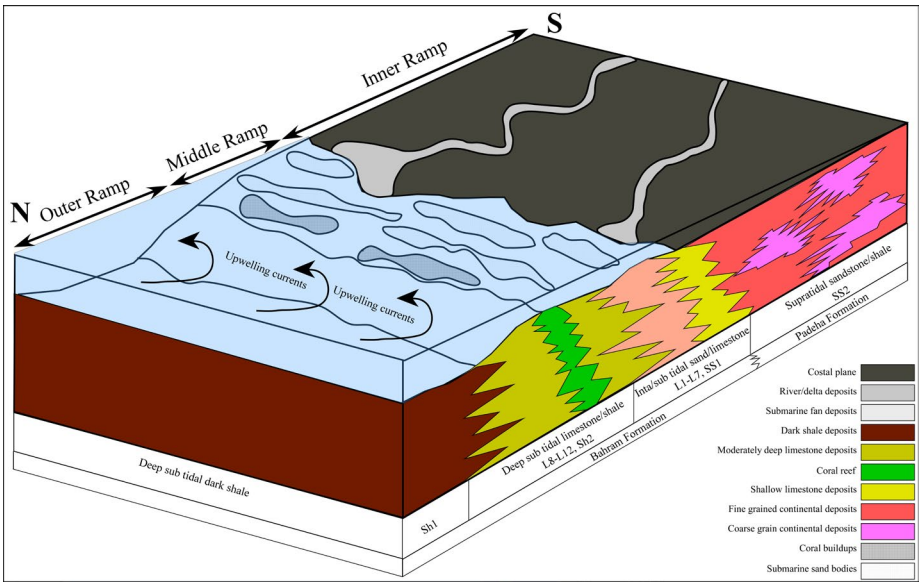

Fig. 3 - Conceptual block diagram of the suggested sedimentary model for the studied strata.

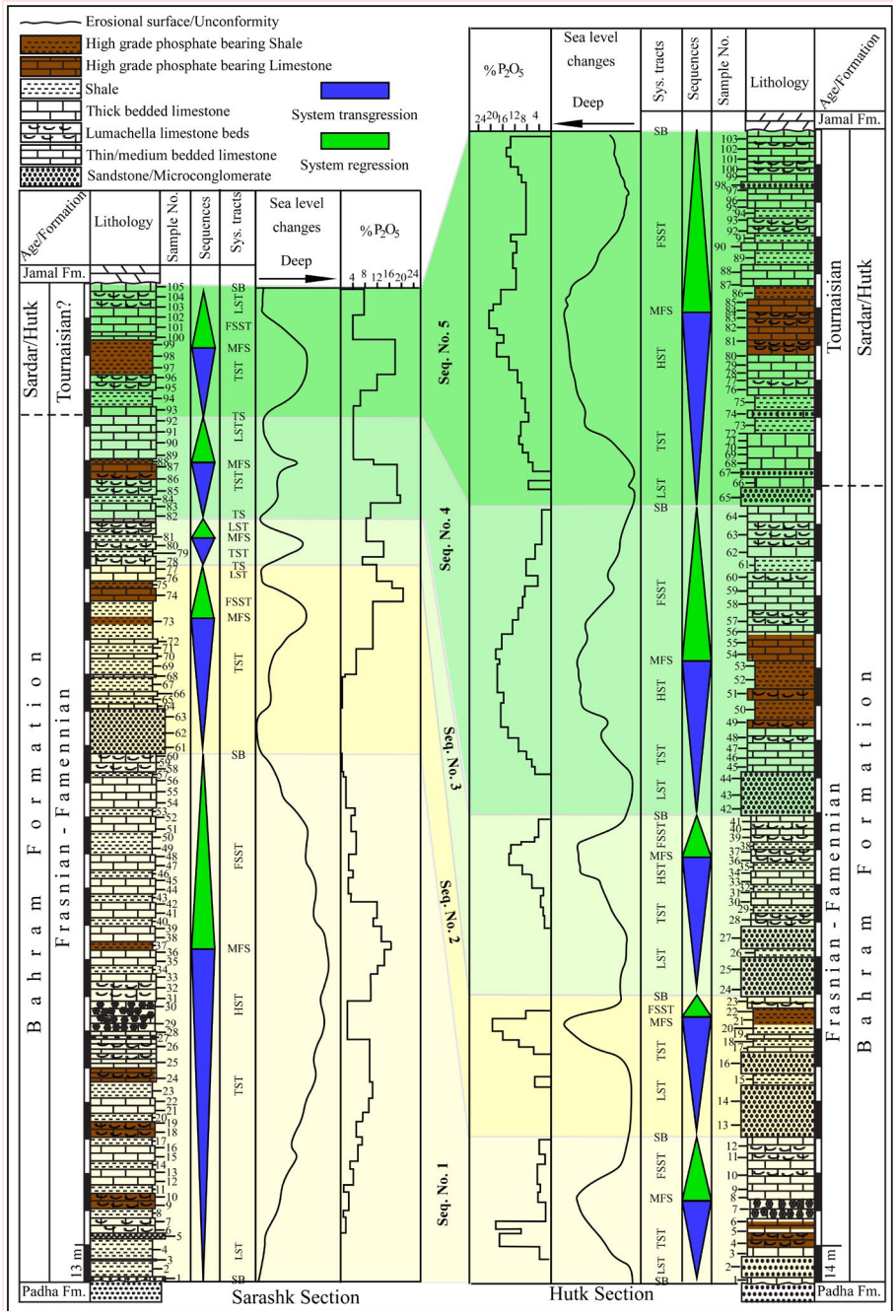

Fig. 4 - The sequence stratigraphy of the studied sections, sea level fluctuations and changes in phosphate content.

ed barrier reefs, and an absence of turbidities and lateral changes in sedimentary layers. These suggest a mixed carbonate-siliciclastic ramp sedimentary environment. This sedimentary environment is emphasized in the Hutk section (Hashmie et al. 2016) and in the whole area (Wendt et al. 2002). This sedimentary environment consists of supratidal and near-shore facies belt, inner ramp, middle ramp and outer ramp facies zones (Fig. 3).

Despite of different thickness, the major facies and lithology changes are similar in both sections. Based on the lithology and facies changes, five sedimentary sequences have distinguished in studied sections. The first sequence is more remarkable in the Sarashk Section (Fig. 4) and mainly includes shallow clastic facies at the base and marine carbonate and shale strata in the middle and upper parts. In both sections, this sequence starts by shallow marine and near shore clastic deposits that point to the low stand system tract (LST), (Fig. 5a, b). This is followed by deepening upward deposits; including major limestone layers and minor shale intercalations. At the base of the first sequence, clastic and carbonate deposits of near shore and supratidal environments gradually changed into middle - outer ramp, which indicate the transgressive system tract

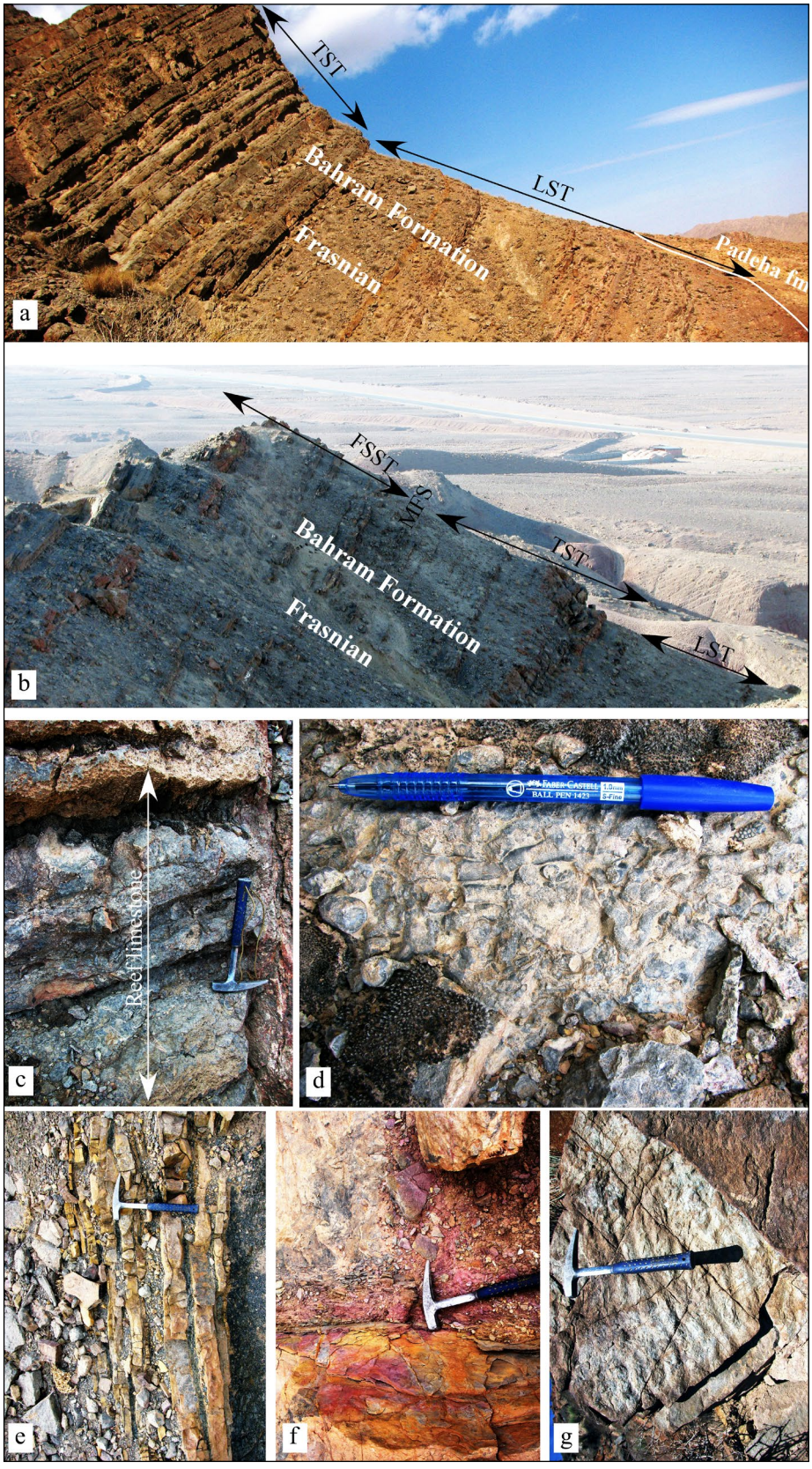

Fig. 5 - a) The lower part of the first sequence in the Sarashk Section; b) the whole exposure of the first sequence in the Hutk Section; c) the outcrop of the reef limestone in the Sarashk section; d) a closer view of the reef limestone in the Sarashk Section; e) fine shale/limestone succession in the HST succession of the first sequence; f) the erosional surface at the top of the first sequence in the Hutk Section; g) the coastal ripple marks at the top of the first sequence in the Sarashk Section.

(TST). In both sections, the deepest part of this sequence is in the shale and dark limestone strata that were deposited after a remarkable coral reef facies (Figs. 5c, d). In both sections, fine limestone – dark shale intercalations (Fig. 5e) were deposited after the TST that indicate the high stand system tract (HST). In the Sarashk Section, an organic rich phosphate bearing black shale (facies Sh1) indicates the

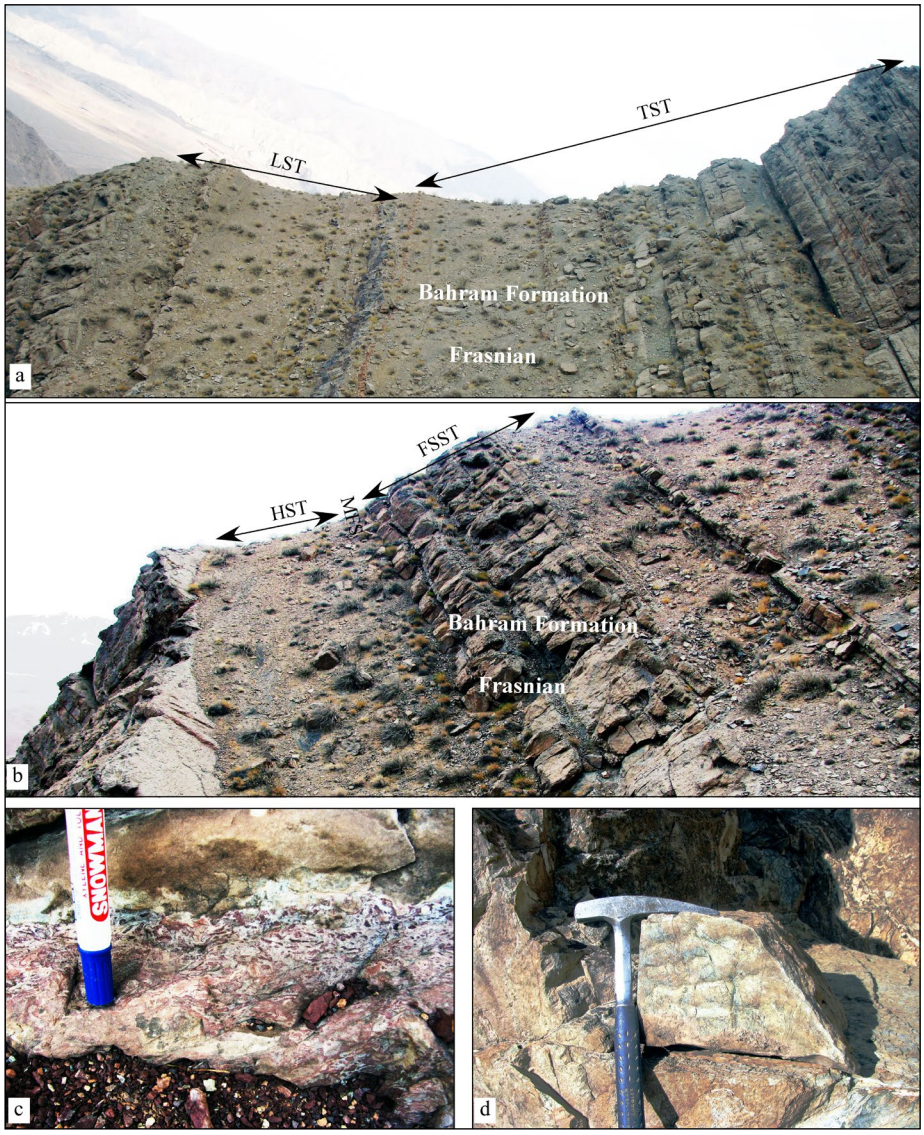

Fig. 6 - a) The lower part of the second sequence in the Sarashk Section; b) the upper part of the second sequence in the Sarashk Section; c) the Skolithos/Glossifungites trace facies at the top of the second sequence in the Sarashk Section; d) the coastal ripple marks at the base of the third sequence in the Sarashk section.

maximum flooding surface (MFS), but in the Hutk section, the microfacies L12 (table 2) is dominant and points to MFS. The upper half of the sequence comprises shallowing upward deposits, from outer ramp to near shore deposits, and indicates the falling stage system tract (FSST). The top of the first sequence in both sections is characterized by an erosional surface (i.e. a Sequence boundary, SB1) and a minor paleosol horizon, especially in the Hutk Section (Fig. 5f). As well as an erosional surface, some coastal ripple marks are recorded on the top of the first sequence in the Sarashk section (Fig. 5g).

The second sequence, like the first one, starts by shallow clastic deposits of the supratidal zone that correspond to the LST, and most of the lower half of this sequence consists of transgressive marine strata (TST), (Fig. 6a). In both sections, a relatively thick black organic rich shale reflects the maximum sea level rise and points to the MFS/HST. The upper part of this sequence shows a short interval of FSST, which is terminated by a shallow marine environment (Fig. 6b). The upper boundary of this sequence in the Sarashk Section is marked by a horizon that includes burrowing traces of Skolithos/Glossifungites trace facies (Fig. 6c) indicating a long period of low stand (SB1). In the Hutk Section, this sequence ends with the basal supratidal clastic deposits of the next sequence (SB1) (Fig. 6d).

The third sequence is ~ 70m thick in the Hutk Section and is lithologically similar to the second one (Fig. 7a); but it is condensed to ~ 15 m thick in the Sarashk Section (Fig. 7b). A short period of sea level rise led to the deposition of an onlap transgressive succession (TST), which is topped by a dark organic rich shale as MFS/HST. This peri-

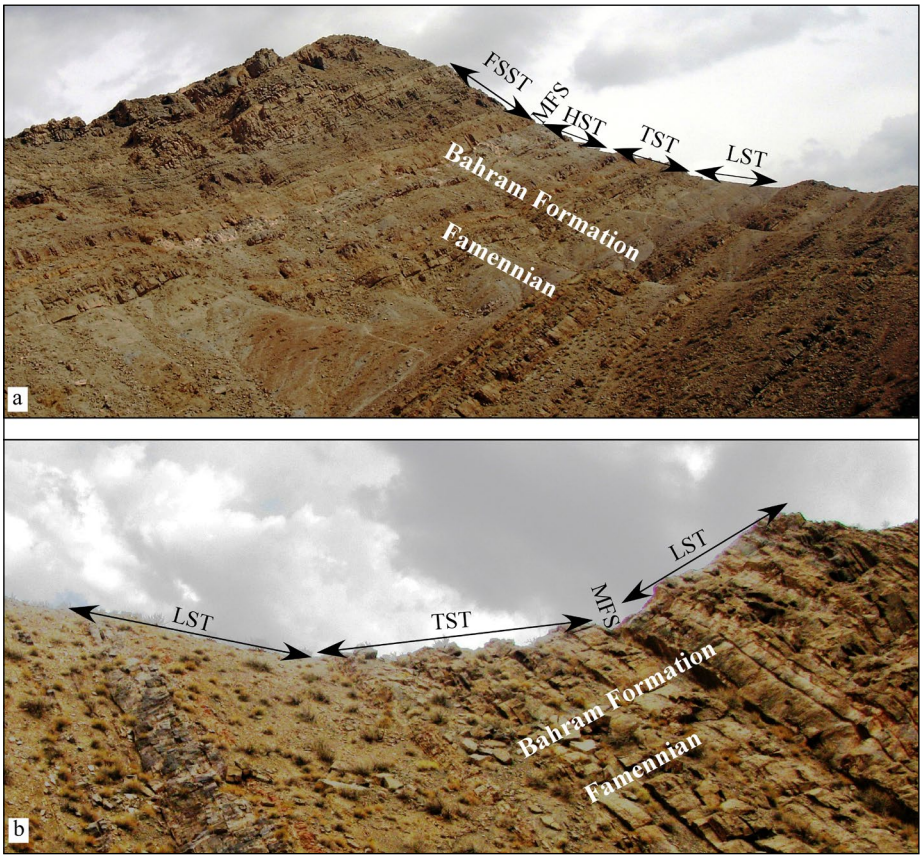

Fig. 7 - a) The exposure of the third sequence in the Hutk Section; b) the exposure of the third sequence in the Sarashk section.

od of transgression and flooding was followed by rapid regression and facies change from deep outer ramp to the shallow inner ramp (FSST). However, in both sections, this sequence starts with shallow supratidal and intertidal deposits and is followed by deepening upward facies, a short HST is recorded as shale and limestone intercalations, the MFS/HST is marked by a black shale layer, which follows by a shallowing upward succession to near shore clastic deposits. The basal and top boundaries of the third sequence in the Hutk Section is marked as a type 1 sequence boundary (SB1) but in the Sarashk Section it is marked by transgressive surfaces as a type 2 sequence boundary (SB2).

The fourth and fifth sequences in both sections are similar to the third one in each section and more remarkable in the Hutk Section.

Geochemistry

The geochemical analyses show that the phosphate bearing layers in the studied sections contain 10-23% P_2O_5 and include three types. The first type involves fossiliferous limestone strata (Fig. 8 a-c). The most common fauna in these layers are Brachiopods and teeth and rare skeletal plates of fishes (Fig. 8 d-f). The fossil fishes of the studied section mainly include Chondrichthyes (protacrodontids, phoebodontids, cladodontids) (Ahmadi et al. 2006). The average of 12 % and a maximum of 18% P_2O_5 is recorded for these layers. The sequence stratigraphic setting of this type is the TST. In the Hutk section, this type is recorded in the first, fourth and fifth sequences as thick lumachella layers with non-fossiliferous limestone and shale intercalations. In the Sarashk section, this type of phosphate-bearing layer is recorded in the first and fourth sequences with the same lithology as the Hutk Section. The common microfacies of this type include L3, L4 & L5 (Fig. 8 g-i).

The second type of phosphate bearing layer involves the facies of the HST and MFS settings and mainly includes black organic rich shale and limestone strata (Fig. 9 a-d). This type of phosphate-bearing layer is recorded in the second, fourth and fifth sequences in the Hutk Section and in the first, second, fourth and fifth sequence in the Sarashk Section. The phosphate content of these phosphate bearing layers is 10-23% P_2O_5 (average is 18% P_2O_5). In these layers, phosphate occurs as peloids and in shell debris of inarticulate Brachiopoda and Crinoidea (L11 microfacies), (Fig 9 e-g).

The third type of phosphorites occurs just af-

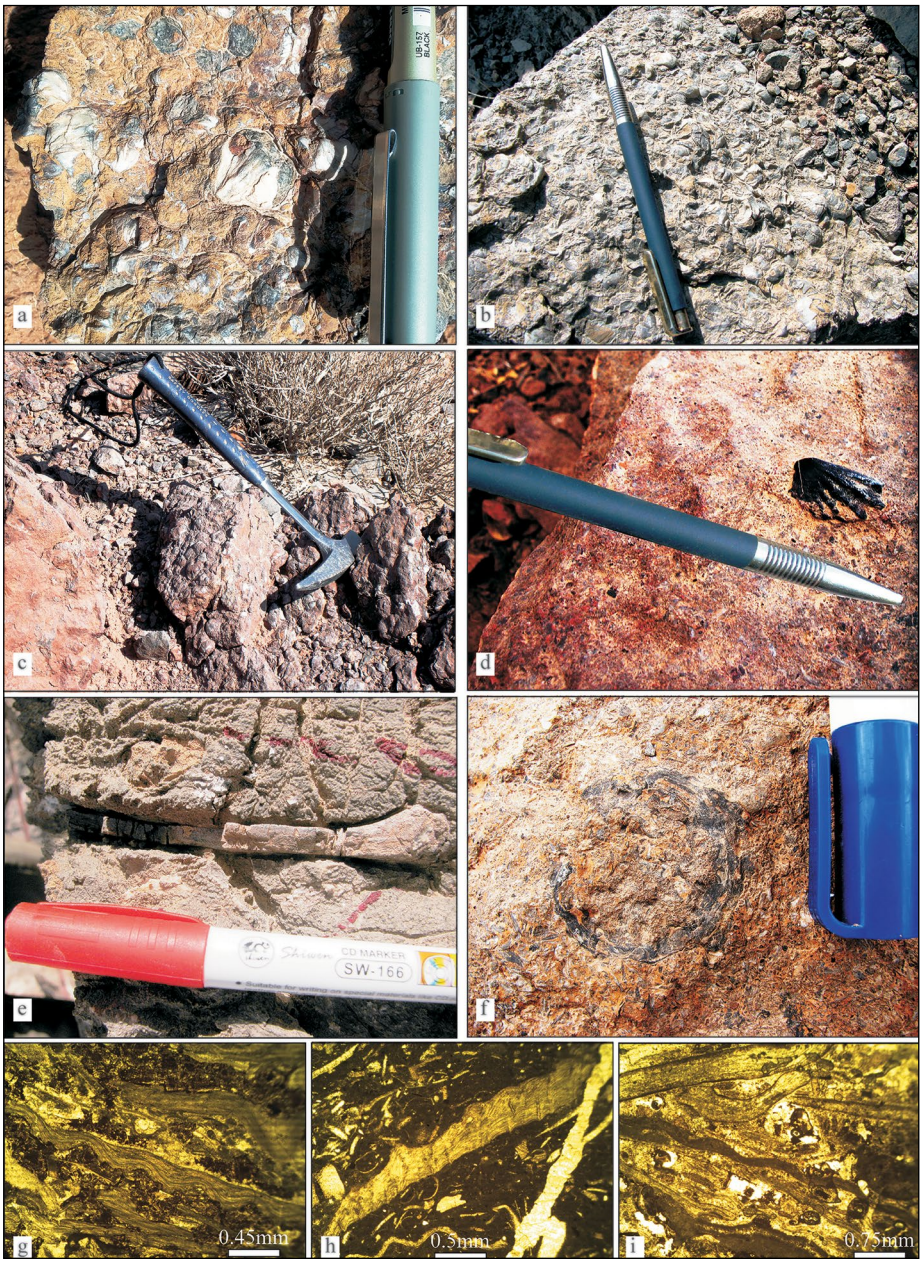

Fig. 8 - a-c) Fossiliferous phosphate bearing limestone strata in the studied sections, a & b, Sarashk Section; c, Hotk section; d, Dipnoi tooth plate in the first type of phosphate bearing layers in the Sarashk Section; e, a cast of an armor plaque in the first type of phosphate bearing layers in the Sarashk Section; f; a cast of an armor plaque in the first type of phosphate bearing layers in the Hutk Section; g, the microphotograph of the L3 microfacies; h, the microphotograph of the L4 microfacies; i, the microphotograph of the L5 microfacies.

ter the MFS at the beginning of sea level fall in the FSST. This type of phosphorite is recorded in the Second and fifth sequences in the Sarashk Section and second, fourth and fifth sequences in the Hutk Section. In this type, the P_2O_5 has mainly reserved in a dark mixture of iron oxide-phosphate cement (Fig. 10 a-d). The phosphatic matrix occurs mainly in L6, L7 & L8 microfacies (Fig. 10 e-g) with intercalations of the Sh2 facies. A maximum of 20% and the average of 15% P_2O_5 is recorded in these layers.

As outlined above (see introduction), upwelling currents are known as the main mechanism for phosphate accumulation in continental margin sediments (McKelvey 1967; Burnett 1977; Lucas & Prevot-Lucas 1977; Baturin 1982; Goldhammer et al. 2010; Grunert et al. 2010; Lass et al. 2010; Goldhammer et al. 2011; Alsenz et al. 2015; Salama et al. 2015; Brandano et al. 2016; Lomnitz 2017; Salama et al. 2018). The amount of P which can be transferred from deep oceans to the surface by upwelling currents is 95% more than found in normal surface waters (Föllmi 1996). The subsequent high productivity, which occurs during upwelling current activity, is followed by toxic waters, anoxia and high mortality in the continental margin's benthic and pelagic communities. In a general context, the production of organic matter and lack of oxygen results in the accumulation of organic matter in continental margin's deposits in upwelling settings (Hu 1984; Pang & Hu 2002). The concentrated organic mass may

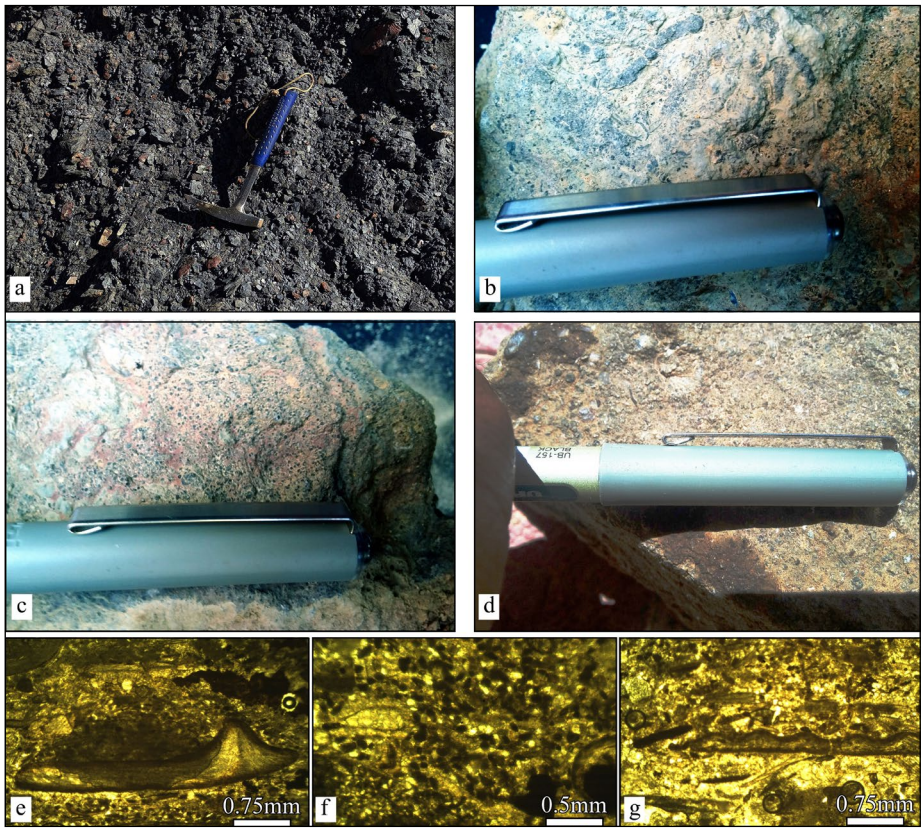

Fig. 9 - a) The exposure of the phosphate bearing dark shale in the Sarashk section; b-d) the filed view of the L11 microfacies, b, Hutk section, c & d, Sarashk section; e-g) microphotographs of the L11 microfacies were prepared from b-d respectively.

be severely affected by post depositional events, especially diagenesis and erosion by sea level changes, and the density of the materials may increase (Salama et al. 2018). However, upwelling currents are mostly active in the open oceans and affect the continental margins along them. The paleogeographic

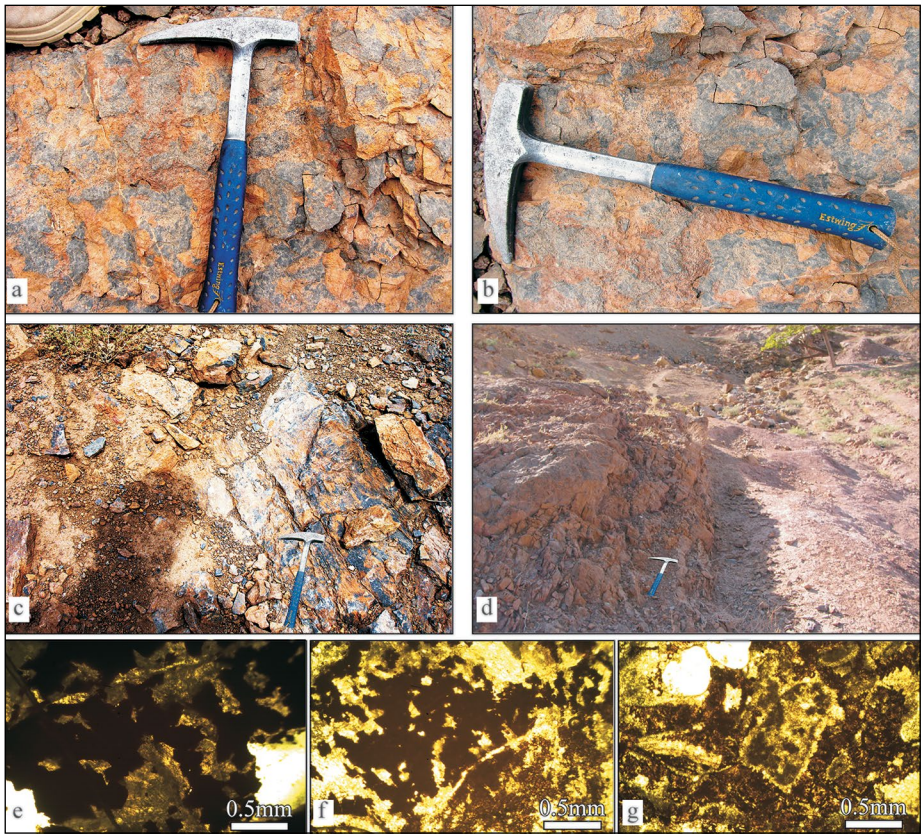

Fig. 10 - a-d) The exposure of the third type of phosphorites, a-b, in the Sarashk Section, c-d in the Hutk Section; e) the microphotograph of the phosphatic cement in the L6 microfacies; f) the microphotograph of the phosphatic cement in the L7 microfacies; g) the microphotograph of the phosphatic cement in the L8 microfacies.

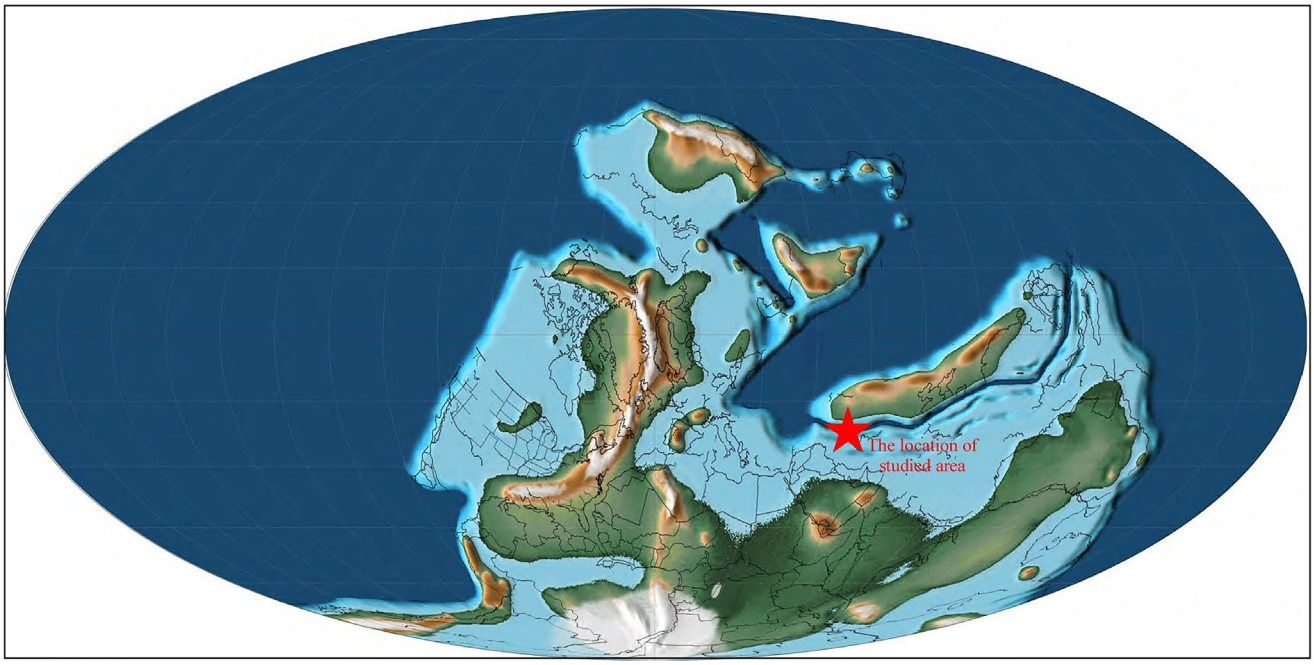

Fig. 11 - Paleogeographic setting of the studied area along the northern margin of the Gondwanaland during the Early Silurian to Carboniferous – Permian Boundary. Modified after Scotese (2014).

position of the studied area, along the northern margin of the Gondwanaland and southern coast of the Paleo-Tethys (Fig. 11), was a favorable setting for upwelling currents at least from the early Silurian to Permo-Carboniferous boundary.

In the case of the studied area, the first phosphorite type is hosted in fossiliferous limestone strata. In some layers, more than 85% of layer volume consists of brachiopoda and other fossils, this concentration mainly resulted in favorable trophic levels which have been resulted by the upwelling current along the continental margin (Fig. 12A). This is a common phenomenon not only during Devonian time (Humphreys & Smith 1989; Giles et al. 2002; Manda & Frýda 2010; Schoepfer et al. 2012; Zambito et al. 2012; Schoepfer et al. 2013; Königshof et al. 2017), but also during the Mesozoic, Cenozoic (Berger et al. 1989; Föllmi et al. 1992; Dornbos 2010; Diedrich 2012; Eoff 2012; Abed 2013), present (Michel et al. 2011) and earlier in the Proterozoic (Khan et al. 2012; Lepland et al. 2013; Hiatt et al. 2015) in the upwelling affected area. Taphonomically, the preservation of this huge amount of shells also points to high productivity and biodiversity formed by upwelling currents (Dornbos 2010; Hendy 2011). The sequence stratigraphic setting of these phosphorites is TST, which mainly points to the sea level rise and increases in the accommodation and accumulation synchronously that led to the accumulation of huge mass of sediments (Föllmi et al. 1992; Abed et al. 2007).

The lithology and sequence stratigraphic setting (HST & MFS) of the second type of phosphorite suggests a moderately deep-water depositional environment. This type of organic rich deposit accumulated on the continental rise and deep open marine basins, near the upwelling affected continental margins (Fig. 12B) (Glenn 1990; Föllmi et al. 1992; Giles et al. 2002).This type of organic rich deposit accumulated on the continental rise and deep open marine basins, near the upwelling affected continental margins (Fig. 12B) (Glenn 1990; Föllmi et al. 1992; Giles et al. 2002). This type of phosphorite contains phosphatic peloids as the main phosphate component. Similar phosphorite deposits have been reported from the Mediterranean region (Abed 2013) and South Africa (Birch 1979). The phosphatic peloids may have different sizes and origins, the main mechanisms of their formation are growth around foreign grains (as coated grains), phospho-micritization of bone and shell fragments, fragmentation and abrasion of intraclasts, pelletization of aggregates and phosphatization and fragmentation of faecal pellets (Emigh 1956; Soudry & Nathan 1980; Salama et al. 2015). On the other hand, geochemical analyses indicate that these phosphorites are the most economically viable and recoverable in the studied sections. As

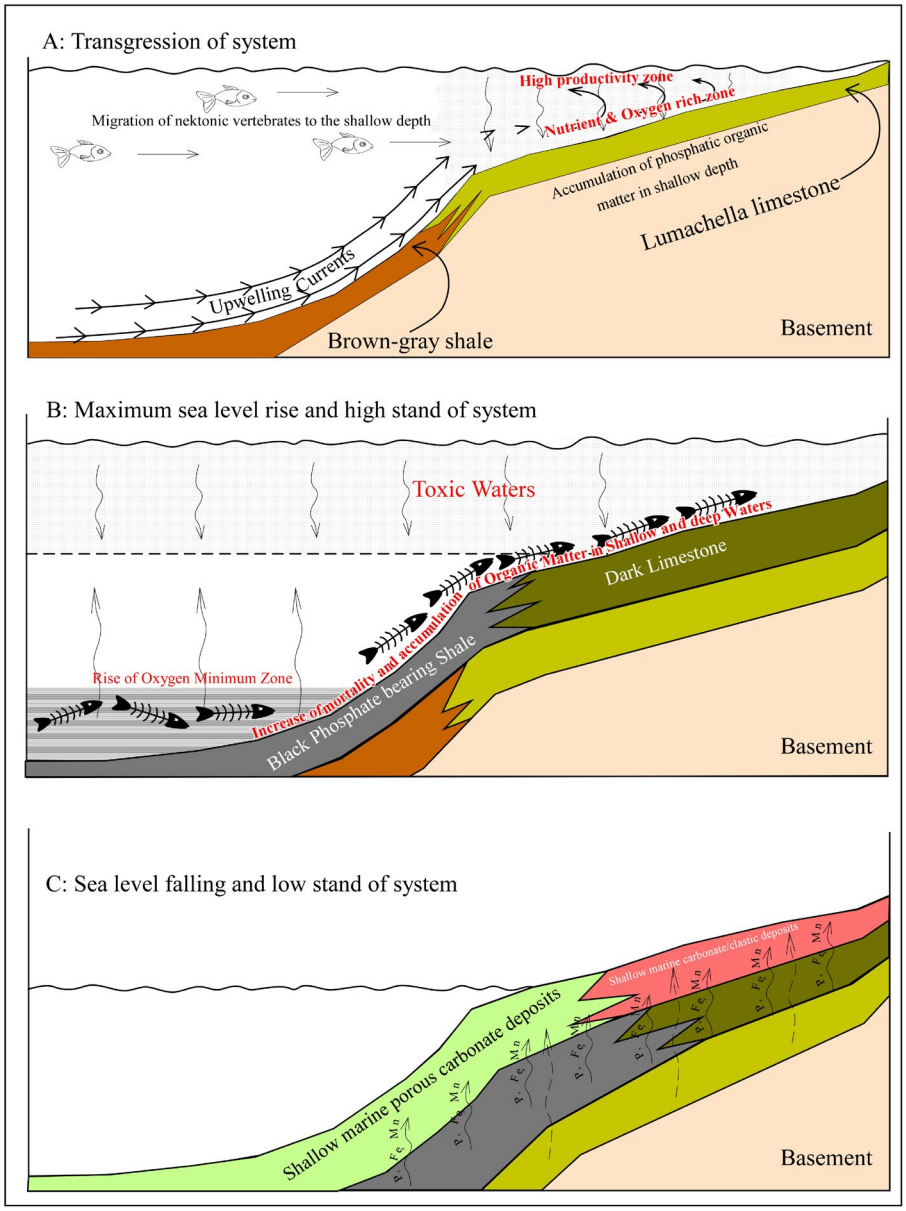

Fig. 12 - Conceptual model for phosphate factories in the studied section; A) the deposition of first phosphorite type during the TST as a result of upwelling currents. B) the deposition of second phosphorite type during the HST setting as a result of high productivity and OMZ rise. C) the deposition of phosphatic cement in the FSST deposits, as a result of pore water migration from phosphate rich underlying sediments during burial digenesis and subsequent cementation.

a brief context, almost all dark shale strata in the studied sections are phosphate-bearing and many of them could be used as phosphate resources and commercially valuable. The dark color of these deposits and lack of benthic creatures are the results of the rise of oxygen minimum zone (Brasier 1980; Loughman & Hallam 1982; Petsch & Berner 1998; Schenau et al. 2000) which commonly occurs in deep waters in upwelling settings (Goldhammer et al. 2011; Lomnitz 2017). In this phosphorite type, higher manganese concentration is recorded too, which emphasizes the near upwelling setting (Cox & Singer 1986), and the presence of the MnO enhanced the dark and black color of these strata.

The third and the most complicated phosphorite type, which occurs in the falling stage system tract as a mixture of FeO and P_2O_5 cement, may have resulted from post-depositional events. The cementation during digenesis is a result of a complicated series of events. The migration of pore water, Eh and pH changes, temperature fluctuations and static water table rise and fall may resulted to the crystallization or dissolution of cement (Mackenzie 2005). Therefore, the third phosphorite type may be completely diagenetic and deposited after sedimentation during the burial history of the successions. This type is similar to the phosphorite deposits in northern Iran described by Salama et al. (2018). In fact, the deposits of the second phosphorite type in the studied strata were the phosphorous source for the third type. In this scenario, during the burial stage, the porous texture of the L6, L7 & L8 mi-

crofacies was a favorable setting for the discharged pore waters from the underlying phosphate-bearing shales. This pore water migration carries P, Fe, Mn and Mg from fine-grained HST and MFS facies to the deposits of the FFST and phosphate rich cements are deposited (Fig. 12C). In this case, just immediately adjacent upper strata of the second phosphorite type (basal layers of the FFST setting) are affected.

The same phosphorite factories in the Phanerozoic are common (Dornbos 2010) and have been reported from Antarctica (Cathcart & Schmidt 1977), China (Kametaka et al. 2005), British Columbia and terrane accretion to western North America (Poulton & Aitken 1989), Jordan (Pufahl et al. 2003), India (Rao et al. 1993), Panthalassa Ocean at the Permian–Triassic Boundary (Schoepfer et al. 2012), Turkey (Sheldon 1964), West Africa (Slansky et al. 1980), Morocco (Trappe 1992), Poland (Trela 2003), Sierra Nevada Range (Varga 1982), and Turkey (Varol 1989).

Furthermore, the compilation of the data of 1600 phosphate mines, deposits and anomalies also shows that the continental margins of Gondwanaland have been the sites of phosphate accumulation (Chernoff & Orris 2002). These deposits know are known in western US (Hein et al. 2004) and worldwide (Orris & Chernoff 2004).

Conclusions

To consider the Devonian phosphate rich deposits in the north of Kerman for industrial uses, reported by several authors (Dimitrijevic 1973; Dastanpour 1996, 1999; Wendt et al. 2002), detailed microfacies and geochemical analyzes were done. The microfacies analyses of the Hutk and Sarashk sections indicate that the bulk succession consists of limestones, shales and sandstones. The limestone lithofacies is classified into 12 microfacies (L1-L12), the shale lithofacies includes 2 facies (Sh1 and Sh2) and the sandstone lithofacies consists of 2 microfacies (Ss1 and Ss2). The lateral changes and relations of these lithofacies and microfacies suggest a mixed carbonate siliciclastic ramp as the depositional model for the studied strata.

Based on the sea level changes and microfacies analysis, five sedimentary sequences could be distinguished in both sections. The first and second ones are most remarkable in the Sarashk Section and the third, fourth and fifth ones are more remarkable in the Hutk section.

The identified sequences in the Hutk Section are normal; these sequences start by shallow deposits of the supratidal and near-shore deposits, followed by transgressive (TST) deposits up to the HST and MFS settings and terminated by shallowing upward deposits (FSST setting), the boundary of all sequences in this section is sharply recorded as SB1. In the Sarashk Section, the first and second sequences are similar to the Hutk section but the third, fourth and fifth sequences are distinguished by detailed microfacies analyses and the sequence boundaries are recorded as transgressive surfaces (SB2). The phosphorite layers in the studied section include three types; the first type involves TST deposits and is a direct result of upwelling currents and high productivity and accumulation of brachiopoda shells and fish teeth and plaque. The second and the most economically viable type is found in HST and MFS settings and seems to be the result of the rise of oxygen minimum zone and accumulation of organic mass at the sea bottom. The third type is found in FSST settings and is a result of diagenesis and cementation processes.

Acknowledgments: Authors are thankful to the Institute of Science and High Technology and Environmental Sciences, Graduate University of Advanced Technology that supports this study as the research project No. 94/5282. Authors thank also referees and the Editorial Board of RIPS.

References

Abed AM. (2013) - The eastern Mediterranean phosphorite giants: An interplay between tectonics and upwelling. *GeoArabia,* 18: 67-94.

Abed AM., Sadaqah R. & Al-Jazi M. (2007) - Sequence stratigraphy and evolution of Eshidiyya phosphorite platform, southern Jordan. *Sedimentary Geology,* 198: 209-219.

Adorno R.R., Silva L.G.D., Buch T., Bahia R.B.C. & Almeida M.E. (2016) - New sedimentary phosphate occurrences in the Parecis Basin, State of Rondônia, Brazil: results, perspectives and preliminary interpretations. *CPRM Geological Survey of Brasil Technical Report*, 4: 1-6.

Ahmadi T., Dastanpour M. & Vaziri MR. (2011) - Upper Frasnian (Upper Devonian) *Polygnathus* and *Icriodus* conodonts from the Bahram Formation, Hur Section, Kerman Province, southeastern iran. *Rivista Italiana di Paleontologia e Stratigrafia,* 118: 203-212.

Ahmadi T., Dastanpour M, Vaziri MR. & Bahrami A. (2016) - Biostratigraphy and Paleoecology of Lower Carbonif-

erous Strata in Hutk Section (Kerman) Based on Conodonts. *Sedimentary Facies,* 9: 1-12 (In Persian with English abstract).

Ahmadi T., Hairapetian V., Gholamalian H., Vaziri MR. & Dastanpour M. (2006) - Late Devonian-Early Carboniferous fish microremains from Kerman. *Geosciences Quarterly Journal,* 100: 131-142.

Alsenz H.. Illner P., Ashckenazi-Polivoda, S., Meilijson, A., Abramovich S., Feinstein S., Almogi-Labin A., Berner Z. & Puttmann W. (2015) - Geochemical evidence for the link between sulfate reduction, sulfide oxidation and phosphate accumulation in a Late Cretaceous upwelling system. *Geochemical Transactions.* 16(2): 1-13.

Bahrami A., Gholamalian H., Corradini C. & Yazdi M. (2011) - Upper Devonian conodont biostratigraphy of Shamsabd Section, Kerman Province, Iran. *Rivista Italiana di Paleontologia e Stratigrafia,* 117: 199-209

Bahrami A., Zamani F., Corradini C., Yazdi M. & Ameri H. (2014) - Late Devonian (Frasnian) conodonts from the Bahram Formation in the Sar-e-Ashk Section, Kerman Province, Central-East Iran Microplate. *Bollettino della Società Paleontologica Italiana,* 53: 179-188.

Bailey JV., Corsetti FA., Greene SE., Crosby CH., Liu P. & Orphan VJ. (2013) - Filamentous sulfur bacteria preserved in modern and ancient phosphatic sediments: implications for the role of oxygen and bacteria in phosphogenesis. *Geobiology,* 11: 397-405.

Bailey JV., Joye SB., Kalanetra KM., Flood BE. & Corsetti FA. (2007) - Evidence of giant sulphur bacteria in Neoproterozoic phosphorites. *Nature,* 445: 198-201.

Barale L., D'Atri A. & Martire L. (2013) - The Role of Microbial Activity In the Generation of Lower Cretaceous Mixed FE-Oxide-phosphate Ooids from the Provencal Domain, French Maritime Alps. *Journal of Sedimentary Research,* 83: 196-206.

Baturin GN. (1982) - Phosphorites on the sea floor, origin, composition and distribution, Developments in Sedimentology vol 33. Elsevier, New York, 343 pp.

Berberian M. & King GCP. (1981) - Towards a paleogeography and tectonic evolution of Iran. *Canadian Journal of Earth Sciences,* 18: 210-265.

Berger WH., Smetacek VS. & Wefer G. (1989) - Ocean productivity and paleoproductivity - An overview. In: In: Berger H., Smetacek VS. & Wefer G. (Eds) - Productivity of the ocean: present and past, vol 44. Wiley, New York, pp 1-34.

Berner RA. (1973) - Phosphate removal from sea water by adsorption on volcanogenic ferric oxides. *Earth and Planetary Science Letters,* 18: 77-86.

Birch GF. (1979) - Phosphorite pellets and rock from the western continental margin and adjacent coastal terrace of South Africa. *Marine Geology,* 33: 91-116.

Brandano M., Westphal H., Mateu-Vicens G., Preto N. & Obrador A. (2016) - Ancient upwelling record in a phosphate hardground (Tortonian of Menorca, Balearic Islands, Spain). *Marine and Petroleum Geology,* 78: 593-605.

Brasier MD. (1980) - The Lower Cambrian transgression and glauconite-phosphate facies in western Europe. *Journal of Geological Socity of London*, 137: 695-703

Burnett WC. (1977) - Geochemistry and origin of phosphorite deposits from off Peru and Chile. *Geological Society of America Bulletin,* 88(6): 813-823.

Cathcart JB. & Schmidt DL. (1977) - Middle paleozoic sedimentary phosphate in the Pensacola Mountains, Antarctica. *Geological Survey Professional Paper*, 456: 1-24.

Chernoff CB. & Orris GJ. (2002) - Data Set of World Phosphate Mines, Deposits, and Occurrences—Part A. Geologic Data. US Geological Survey, New York, 352 pp.

Cook PJ. & Mc Elhinny MW. (1979) - A reevaluation on the Spatial ndd temporal distribution of sedimentary Phosphate deposits in the Light of Plate Tectonics. *Economic Geology*.74: 315-330.

Cox DP. & Singer DA. (1986) - Mineral deposit models. *US Geological Survey Bulletin*, 1693: 1-379.

Dastanpour M. (1996) - The Devonian System in Iran: a review. *Geological Magazine*, 133: 159-170.

Dastanpour M. (1999) - The stratigraphy and geochemistry of Late Devonin phosphatic rocks in Kerman. *Research Journal of University of Isfahan*, 13: 72-59 [In Persian with English abstract].

Diedrich CG. (2012) - Eocene (Lutetian) Shark-Rich Coastal Paleoenvironments of the southern North Sea Basin in Europe: Biodiversity of the Marine Fürstenau Formation Including Early White and Megatooth Sharks. *International Journal of Oceanography*, 2012: 1-22.

Dimitrijevic MD. (1973) - Geology of Kerman Region vol Yu/52. Geological Survay of Iran, Tehran, 334 pp.

Dornbos SQ. (2010) - Phosphatization Through the Phanerozoic. In: Taphonomy: 435-465. Springer, Dordrecht.

Emigh GD. (1956) - The petrography, mineralogy, and origin of phosphate pellets in the western Permian formation and other sedimentary formations. PhD thesis, the University of Arizona, 377 pp.

Eoff JD. (2012) - Correlation of resource plays and biodiversity patterns: Accumulation of organic-rich shale tracks taxonomic turnover. *Gulf Coast Association of Geological Societies*, 1: 1-12.

Flügel E. (2010) - Microfacies of Carbonate Rocks (Analysis, Interpretation and Application). Second edn. Springer, Berlin, 1006 pp.

Flügel E. (2012) - Microfacies analysis of limestones. Springer Science & Business Media, Berlin, 633 pp.

Föllmi KB. (1996) - The phosphorus cycle, phosphogenesis and marine phosphate-rich deposits. *Earth-Science Reviews,* 40: 55-124.

Föllmi KB., Garrison RE., Ramirez PC., Zambrano-Ortiz F., Kennedy WJ. & Lehner BL. (1992) - Cyclic phosphate-rich successions in the upper Cretaceous of Colombia. *Palaeogeography, Palaeoclimatology, Palaeoecology,* 93: 151-182.

Froelich PN., Bender ML., Luedtke NA., Heath GR. & DeVries T. (1982) - The marine phosphorus cycle. *American Journal of Science*, 282: 474-511.

Gholamalian H. (2006) - Biostratigraphy of Late Devonian Sequence in Hutk Section (North of Kerman) Based on Conodonts. *Geosciences Quarterly Journal*, 59: 94-101 [In Persian with English abstract].

Gholamalian H., Ghoreishi-Maremy S. & Parvaneh Nejad Shirazi M. (2014) - Biostratigraphy of Late Devonian Conodonts in Gerik Section, Eastern Zarand (Kerman Province). *Geosciences Quarterly Journal*, 23: 105-115 [In Persian with English abstract].

Gholamalian H., Hairapetian V., Barfehei N., Mangelian S. & Faridi P. (2013) - Givetian-Frasnian boundary conodonts from Kerman Province, Central Iran. *Rivista Italiana di Paleontologia e Stratigrafia*, 119: 133-146.

Gholamalian H. & Kebriaei MR. (2008) - Late Devonian conodonts from the Hojedk Section, Kerman Province , southeastern Iran. *Rivista Italiana di Paleontologia e Stratigrafia*, 114: 179-189.

Gholamalian H., Sajadi SH. & Hassani MJ. (2015) - Biostratigraphy of Devonian succession (Bahram Formation) in Sardar section, North of Kerman based on conodonts. *Paleontology*, 2(2): 198-215 [In Persian with English abstract].

Giles KA., McMillan NJ. & McCarson BL. (2002) - Geochemical analysis and paleoecological implications of phosphatic microspherules (otoliths?) from Frasnian-Famennian boundary strata in the Great Basin, USA. *Palaeogeography, Palaeoclimatology, Palaeoecology,* 181(1-3): 111-125.

Glenn CR. (1990) - Depositional sequences of the Duwi, Sibaiya and Phosphate Formations, Egypt: phosphogenesis and glauconitization in a Late Cretaceous epeiric sea. *Geological Society of London Special Publications,* 52: 205-222.

Goldhammer T., Brüchert V., Ferdelman TG. & Zabel M. (2010) - Microbial sequestration of phosphorus in anoxic upwelling sediments. *Nature Geoscience,* 3: 557-561.

Goldhammer T., Brunner B., Bernasconi SM., Ferdelman TG. & Zabel M. (2011) - Phosphate oxygen isotopes: Insights into sedimentary phosphorus cycling from the Benguela upwelling system. *Geochimica et Cosmochimica Acta*, 75: 3741-3756.

Grunert P., Soliman A., Harzhauser M., Müllegger S., Piller W., Roetzel R. & Rögl F. (2010) - Upwelling conditions in the Early Miocene Central Paratethys Sea. *Geologica Carpathica,* 61(2): 129-145.

Hashmie A., Rostamnejad A., Nikbakht F., Ghorbanie M., Rezaie P. & Gholamalian H. (2016) - Depositional environments and sequence stratigraphy of the Bahram Formation (middle–late Devonian) in north of Kerman, south-central Iran. *Geoscience Frontiers,* 7: 821-834.

Hein JR., Perkins RB. & McIntyre BR. (2004) - Evolution of thought concerning the origin of the Phosphoria Formation, Western US Phosphate Field. Life cycle of the Phosphoria Formation: from deposition to post-mining environment. *Handbook of geochemistry*, 8: 19-42.

Hendy AJW. (2011) - Taphonomic Overprints on Phanerozoic Trends in Biodiversity: Lithification and Other Secular Megabiases. In: Allison PA. & Bottjer DJ. (Eds.) - Taphonomy - Process and Bias Through Time: 19-77. Springer, Netherlands.

Hiatt EE., Pufahl PK. & Edwards CT. (2015) - Sedimentary phosphate and associated fossil bacteria in a Paleoproterozoic tidal flat in the 1.85Ga Michigamme Formation, Michigan, USA. *Sedimentary Geology,* 319: 24-39.

Hu D. (1984) - Upwelling and sedimentation dynamics - I the role of upwelling in sedimentation in the Huanghai Sea and east of china sea, a discription of general features. *Chinese Journal of Oceanology and Limnology,* 2: 12-19

Humphreys B. & Smith SA (1989) - The distribution and significance of sedimentary apatite in Lower to Middle Devonian sediments east of Plymouth Sound. *Proceedings of the Ussher Society,* 7: 118 - 124

Jarvis I., Burnett W. & Baturin G. (1994) - Geochemistry of phosphorite-state of the art. *Eclogae Geologica Helvetiae,* 87: 643-671.

Jasinski SM. (2016) - Mineral commodity summaries. *US Geological Survey, New York*: 124-125

Kametaka M., Takebe M., Nagai H., Zhu S. & Takayanagi Y. (2005) - Sedimentary environments of the Middle Permian phosphorite–chert complex from the northeastern Yangtze platform, China; the Gufeng Formation: a continental shelf radiolarian chert. *Sedimentary Geology,* 174: 197-222.

Kazakov A. (1937) - The phosphate facies: origin of the phosphorite and the geologic factors of formation of the deposits. *Proc Sci Inst Fertilizers and Insectofungicides,* 145: 1-106

Khan KF., Dar SA. & Khan SA. (2012) - Geochemistry of phosphate bearing sedimentary rocks in parts of Sonrai block, Lalitpur District, Uttar Pradesh, India. *Chemie der Erde - Geochemistry,* 72: 117-125.

Khosravi Z., Hosseininejad SM., Dastanpour M., Gholamalian H. & Torkzadeh Mahani I. (2010) - Sedimentary Environment of Late Devonian deposits in the North -East of Baghin area (West Kerman) based on Litofacies and Conodontfacies. In: The first International Applied Geological Congress, Iran-Mashhad: 214-219 [In Persian with English abstract].

Königshof P., Narkiewicz K., Hoa PT., Carmichael S. & Waters J. (2017) - Devonian events: examples from the eastern Palaeotethys (Si Phai section, NE Vietnam). *Palaeobiodiversity and Palaeoenvironments,* 97: 481-496.

Lass H-U., Mohrholz V., Nausch G. & Siegel H. (2010) - On phosphate pumping into the surface layer of the eastern Gotland Basin by upwelling. *Journal of Marine Systems,* 80: 71-89.

Lepland A., Melezhik VA., Papineau D., Romashkin AE. & Joosu L. (2013) - The Earliest Phosphorites: Radical Change in the Phosphorus Cycle During the Palaeoproterozoic. In: Melezhik, V., Prave, A. R., Hanski, E. J., Fallick, A. E., Lepland, A., Kump, L. R., & Strauss, H. (Eds.) - Reading the Archive of Earth's Oxygenation: 1275-1296. Springer, Berlin, Heidelberg.

Lomnitz U. (2017) - Biogeochemical cycling of iron and phosphorus under low oxygen conditions. PhD. thesis, Christian-Albrechts-Universität, Kiel, 159 pp.

Loughman DL. & Hallam A (1982) - A facies analysis of the Pucara Group (Norian to Toarcian carbonates, organic-rich shale and phosphate) of central and northern Peru. *Sedimentary Geology,* 23: 161-194.

Lucas J. & Prevot-Lucas L. (1977) - On the Genesis of Sedimentary Apatite and Phosphate-Rich Sediments. In: Paquet H (Eds) - Soils and Sediments: 249-268. Springer, Berlin.

Luternauer J.L. & Pilkey O.H. (1967)-Phosphorite grains: their application to the interpretation of North Carolina shelf sedimentation. *Marine Geology*, 5(4): 315-320.

Mackenzie FT, (2005) - Sediments, Diagenesis, and Sedimentary Rocks. Elsevier, Italy, 446 pp.

Manda Š. & Frýda J. (2010) - Silurian-Devonian boundary events and their influence on cephalopod evolution: evolutionary significance of cephalopod egg size during mass extinctions. *Bulletin of Geosciences,* 85: 513-540.

McKelvey VE. (1967) - Phosphate deposits. *Geological survey Bulletin,* 1252(D): 1-32.

Michel J., Westphal H. & Von Cosel R. (2011) - The Mollusk Fauna of Soft Sediments from the Tropical, Upwelling-Influenced Shelf of Mauritania (Northwestern Africa). *Palaios,* 26: 447-460.

Nelson GJ., Pufahl PK. & Hiatt EE. (2010) - Paleoceanographic constraints on Precambrian phosphorite accumulation, Baraga Group, Michigan, USA. *Sedimentary Geology,* 226: 9-21.

Orris GJ. & Chernoff CB. (2004) - Review of world sedimentary phosphate deposits and ccurrences. In: Heinz JR (Eds)-Life Cycle of the Phosphoria Formation: From Deposition to Post-Mining Environment, vol 8. Handbook of Exploration and Environmental Geochemistry: 599-573. Elsevier, New York.

Pang C-g. & Hu D-x. (2002) - Upwelling and sedimentation dynamics III- Coincidence of upwelling areas with mud patches in north hemisphere shelf seas. *Chinese Journal of Oceanology and Limnology,* 20: 101-106.

Pasek MA. (2008) - Rethinking early Earth phosphorus geochemistry. *Proceedings of the National Academy of Sciences of the United States of America,* 105:853-858.

Petsch ST. & Berner RA. (1998) - Coupling the geochemical cycles of C, P, Fe, and S; the effect on atmospheric O_2 and the isotopic records of carbon and sulfur. *American Journal of Science,* 298: 246-262.

Poulton TP. & Aitken JD. (1989) - The Lower Jurassic phosphorites of southeastern British Columbia and terrane accretion to western North America. *Canadian Journal of Earth Sciences,* 26(8): 1612-1616.

Pufahl PK., Grimm KA., Abed AM. & Sadaqah RMY. (2003) - Upper Cretaceous (Campanian) phosphorites in Jordan: implications for the formation of a south Tethyan phosphorite giant. *Sedimentary Geology,* 161: 175-205.

Pufahl PK. & Groat LA. (2016) - Sedimentary and Igneous Phosphate Deposits: Formation and Exploration: An Invited Paper. *Economic Geology,* 112: 483–516.

Rao VP., Lamboy M. & Dupeuble PA. (1993) - Verdine and other associated authigenic (glaucony, phosphate) facies from the surficial sediments of the southwestern continental margin of India. *Marine Geology,* 111: 133-158.

Reimers C., Kastner M., Garrison R., Burnett W. & Riggs S. (1990) - The role of bacterial mats in phosphate mineralization with particular reference to the Monterey Formation. *Phosphate deposits of the world,* 3: 300-311.

Salama W., El-Kammar A., Saunders M., Morsy R. & Kong C. (2015) - Microbial pathways and palaeoenvironmental conditions involved in the formation of phosphorite grains, Safaga District, Egypt. *Sedimentary Geology,* 325: 41-58.

Salama W., Khirekesh Z., Amini A. & Bafti BS. (2018) - Diagenetic evolution of the upper Devonian phosphorites, Alborz Mountain Range, northern Iran. *Sedimentary Geology,* 376: 90-112.

Schenau SJ., Slomp CP. & De Lange GJ. (2000) - Phosphogenesis and active phosphorite formation in sediments from the Arabian Sea oxygen minimum zone. *Marine Geology,* 169: 1-20.

Schoepfer S.D., Henderson C. M., Garrison G. H., Foriel J., Ward P. D., Selby D., Hower Jc., Algeo TJ. & Shen Y. (2013) - Termination of a continent-margin upwelling system at the Permian–Triassic boundary (Opal Creek, Alberta, Canada). *Global and Planetary Change,* 105: 21-35.

Schoepfer SD., Henderson CM., Garrison GH. & Ward PD (2012) - Cessation of a productive coastal upwelling system in the Panthalassic Ocean at the Permian–Triassic Boundary. *Palaeogeography, Palaeoclimatology, Palaeoecology,* 313-314: 181-188.

Schulz HN. & Schulz HD. (2005) - Large sulfur bacteria and the formation of phosphorite. *Science,* 307: 416-418.

Scotese CR. (2014) - Atlas of Devonian paleogeographic maps. *Paleomap atlas for ArcGIS,* 4: 65-72.

Sheldon RP. (1964) - Exploration for phosphorite in Turkey; a case history. *Economic Geology,* 59: 1159-1175.

Simandl GJ., Paradis S. & Fajber R. (2011) - Sedimentary Phosphate Deposits Mineral Deposit Profile F07. *Geological Fieldwork,* 2012: 217-222.

Slansky M., Sheldon RP. & Burnett WC. (1980) - Ancient upwelling models: Upper Cretaceous and Eocene phosphorite deposits around West Africa. Paper presented at the Fertilizer mineral potential in Asia and the Pacific, Honolulu, Hawaii , USA: 145-158.

Soudry D. & Nathan Y. (1980) - Phosphate peloids from the Negev phosphorites. *Journal of the Geological Society of London,* 137: 749-755.

Swanson R.G. (1981)- Sample examination manual; Methods in Exploration Series; No. 1. AmericanAssociation of Petroleum Geologists, Oklahoma, 135 pp.

Trappe J. (1992) - Microfacies zonation and spatial evolution of a carbonate ramp: marginal Moroccan phosphate sea during the Paleogene. *Geologische Rundschau,* 81: 105-126.

Trappe J. (1998) - Phosphate minerals and sediments. *Lecture Notes in Earth Sciences,* 76: 9-58.

Trela W. (2003) - Sedimentary environment of the Ordovician phosphate–bearing sequence in central Poland (Holy Cross Mts.). *INSUGEO Serie Correlatión Geológica,* 17: 475-481.

Varga RJ. (1982) - Implications of Palaeozoic phosphorites in the northern Sierra Nevada Range. *Natur,* 297(5863): 217-220.

Varol B. (1989) - Sedimentary petrography and origin of phosphate peloids of the Mazidağ-Derik Area (Mardin,

southeast Turkey). *Mineral Resorce Exploration Bulletin*, 109: 65-73.

Wendt J., Kaufmann B., Belka Z., Farsan N. & Bavandpur AK. (2002) - Devonian/Lower Carboniferous stratigraphy, facies patterns and palaeogeography of Iran. Part I. Southeastern Iran. *Acta Geologica Polonica,* 52: 129-168.

Wheat CG., Feely RA. & Mottl MJ. (1996) - Phosphate removal by oceanic hydrothermal processes: An update of the phosphorus budget in the oceans. *Geochimica et Cosmochimica Acta,* 60: 3593-3608.

Wilson JL. (1975) - Carbonate Facies in Geologic History. Springer, New York, 471 pp.

Zambito JJ., Brett CE. & Baird GC. (2012) - The Late Middle Devonian (Givetian) Global Taghanic Biocrisis in its Type Area (Northern Appalachian Basin): Geologically Rapid Faunal Transitions Driven by Global and Local Environmental Changes. In: Earth and Life: 677-703. Springer, Dordrecht.